

Research article

Open Access

Distinct roles of long/short fimbriae and gingipains in homotypic biofilm development by *Porphyromonas gingivalis*

Masae Kuboniwa*¹, Atsuo Amano², Ei Hashino¹, Yumiko Yamamoto¹, Hiroaki Inaba², Nobushiro Hamada³, Koji Nakayama⁴, Gena D Tribble⁵, Richard J Lamont⁶ and Satoshi Shizukuishi¹

Address: ¹Department of Preventive Dentistry, Osaka University Graduate School of Dentistry, Suita-Osaka, Japan, ²Department of Oral Frontier Biology, Osaka University Graduate School of Dentistry, Suita-Osaka, Japan, ³Department of Oral Microbiology, Kanagawa Dental College, Yokosuka-Kanagawa, Japan, ⁴Department of Developmental and Reconstructive Medicine, Nagasaki University Graduate School of Biomedical Sciences, Nagasaki, Japan, ⁵Department of Periodontics, The University of Texas Health Science Center at Houston, Houston, TX, USA and ⁶Department of Oral Biology, University of Florida College of Dentistry, Gainesville, FL, USA

Email: Masae Kuboniwa* - kuboniwa@dent.osaka-u.ac.jp; Atsuo Amano - amanoa@dent.osaka-u.ac.jp; Ei Hashino - hashino@dent.osaka-u.ac.jp; Yumiko Yamamoto - yymmt@dent.osaka-u.ac.jp; Hiroaki Inaba - hinaba@dent.osaka-u.ac.jp; Nobushiro Hamada - hamadano@kdcnet.ac.jp; Koji Nakayama - knak@nagasaki-u.ac.jp; Gena D Tribble - gena.d.tribble@uth.tmc.edu; Richard J Lamont - rlamont@dental.ufl.edu; Satoshi Shizukuishi - shizuku@dent.osaka-u.ac.jp

* Corresponding author

Published: 26 May 2009

Received: 26 December 2008

BMC Microbiology 2009, 9:105 doi:10.1186/1471-2180-9-105

Accepted: 26 May 2009

This article is available from: <http://www.biomedcentral.com/1471-2180/9/105>

© 2009 Kuboniwa et al; licensee BioMed Central Ltd.

This is an Open Access article distributed under the terms of the Creative Commons Attribution License (<http://creativecommons.org/licenses/by/2.0>), which permits unrestricted use, distribution, and reproduction in any medium, provided the original work is properly cited.

Abstract

Background: *Porphyromonas gingivalis*, a periodontal pathogen, expresses a number of virulence factors, including long (FimA) and short (Mfa) fimbriae as well as gingipains comprised of arginine-specific (Rgp) and lysine-specific (Kgp) cysteine proteinases. The aim of this study was to examine the roles of these components in homotypic biofilm development by *P. gingivalis*, as well as in accumulation of exopolysaccharide in biofilms.

Results: Biofilms were formed on saliva-coated glass surfaces in PBS or diluted trypticase soy broth (dTSB). Microscopic observation showed that the wild type strain formed biofilms with a dense basal monolayer and dispersed microcolonies in both PBS and dTSB. A FimA deficient mutant formed patchy and small microcolonies in PBS, but the organisms proliferated and formed a cohesive biofilm with dense exopolysaccharides in dTSB. A Mfa mutant developed tall and large microcolonies in PBS as well as dTSB. A Kgp mutant formed markedly thick biofilms filled with large clumped colonies under both conditions. A RgpA/B double mutant developed channel-like biofilms with fibrillar and tall microcolonies in PBS. When this mutant was studied in dTSB, there was an increase in the number of peaks and the morphology changed to taller and loosely packed biofilms. In addition, deletion of FimA reduced the autoaggregation efficiency, whereas autoaggregation was significantly increased in the Kgp and Mfa mutants, with a clear association with alteration of biofilm structures under the non-proliferation condition. In contrast, this association was not observed in the Rgp-null mutants.

Conclusion: These results suggested that the FimA fimbriae promote initial biofilm formation but exert a restraining regulation on biofilm maturation, whereas Mfa and Kgp have suppressive and regulatory roles during biofilm development. Rgp controlled microcolony morphology and biovolume. Collectively, these molecules seem to act coordinately to regulate the development of mature *P. gingivalis* biofilms.

Background

Porphyromonas gingivalis has been shown to be a major etiologic agent of destructive adult periodontitis, with a significant lifestyle component harbored within the complex multi-species biofilm (dental plaque) that develops along the gingival margins [1]. The bacterium expresses a number of potential virulence factors, such as long (major) and short (minor) fimbriae, lipopolysaccharides (LPS), and proteases [2]. Among these factors, a unique class of cysteine proteinases, termed gingipains, composed of arginine-specific [Arg-gingipain A and B, (RgpA and RgpB, respectively)] and lysine-specific (Kgp) proteases, are implicated in a wide range of both pathological and physiological processes [3]. Proteases can be post-translationally processed for retention on the cell surface or secretion into the extracellular milieu. Rgp enzymes are glycosylated, with their carbohydrate domain containing phosphorylated branched mannans that can contribute to the anchoring of Rgp on bacterial outer membrane [4]. In addition, this phosphorylated branched mannan constitutes an exopolysaccharide that is distinguishable from both LPS and the serotypeable capsule polysaccharides of *P. gingivalis* [4].

The cell-associated gingipains comprise the majority (~80%) of Rgp and Kgp activities, and are reported to be definitive virulence factors that degrade various host proteins, leading to impaired cellular integrity and function [5]. In addition, gingipains can mediate bacterial interactions with host components [6]. Recent findings indicate that gingipains are also involved in biofilm development. Polyphenolic inhibitors of gingipains can prevent not only homotypic (monospecies) biofilm formation by *P. gingivalis* [7], but also synergistic biofilm formation with *Fusobacterium nucleatum* [8]. In addition, an RgpB-deficient mutant of *P. gingivalis* lost the ability to form synergistic biofilms with *Treponema denticola* [9]. A low molecular weight tyrosine phosphatase, Ltp1, was found to be involved in biofilm formation via suppression of exopolysaccharide production and *luxS* expression, as well as dephosphorylation of gingipains [10]. Thus, gingipains and gingipain regulation may be related to exopolysaccharide accumulation. However, the exact role of gingipains in biofilm development remains to be elucidated.

Two distinct fimbria types, long and short fimbriae, are present on the surface of *P. gingivalis* cells [11]. Long fimbriae impact the host immune response by inducing human peripheral macrophages and neutrophils to overproduce several proinflammatory cytokines such as interleukin-1 (IL-1), IL-6, and tumor necrosis factor alpha, through coordinated interactions with pattern-recognition receptors [12]. Long fimbriae were also reported to induce cross-talk between CXC chemokine receptor 4 and

Toll-like receptor 2 in human monocytes and thus undermine host defense [13]. Furthermore, long fimbriae are prominent adhesins that mediate colonization in periodontal tissues and invasion of host cells as well as dysregulation of host cell cycle, which assists *P. gingivalis* in its persistence in periodontal tissues [14,15]. While, the role of short fimbriae in virulence is less well understood, they are necessary for the development of synergistic biofilms between *P. gingivalis* and *Streptococcus gordonii* via a specific interaction with the streptococcal SspB protein [16]. Recently, these two distinct types of fimbriae were reported to function cooperatively in the development of homotypic biofilms of *P. gingivalis* [17]. It was proposed that the long fimbriae were responsible for bacterial attachment to the substrate as well as initiation of colonization, whereas short fimbriae were involved in the formation of microcolonies and biofilm maturation. In that study, it was also shown that short fimbriae promoted bacterial autoaggregation, which was suppressed by the long fimbriae. In contrast, another study showed opposite results, as deletion of short fimbriae enhanced autoaggregation and negligible autoaggregation occurred in the long fimbria mutants tested [18]. Thus, the contextual roles of these fimbria types in biofilm development are unclear, and further study is necessary.

In the present study, we examined the roles of long and short fimbriae as well as Arg- and Lys-gingipains in homotypic biofilm formation by *P. gingivalis* using a series of deletion mutants of strain ATCC33277.

Results

Microstructure of biofilms under nonproliferation condition

First, we evaluated the roles of long/short fimbriae and gingipains in initial attachment and organization of biofilms which is a crucial event in the early phase of biofilm formation [19]. When cultured in TSB as free-living cells, wild type and all mutant strains showed the similar growth rates, as reported in previous study [20]. In contrast, when incubated in PBS for 24 h, wild type and mutants lacking long and/or short fimbriae formed distinct biofilms (Figure 1 and Table 1). Wild type strain 33277 formed biofilms with a dense basal monolayer and dispersed microcolonies. Compared with the wild type, the long fimbria mutant KDP150 formed patchy and sparser biofilms with a significantly greater distance between fewer peaks, although mean peak height was almost the same as that of the wild type strain. In contrast, the short fimbria mutant MPG67 developed cluster and channel-like biofilms consisting of significantly taller microcolonies compared to the wild type. Similar to MPG67, the mutant (MPG4167) lacking both types of fimbriae also formed thick biofilms with significantly taller microcolonies than the wild type. Viability of the

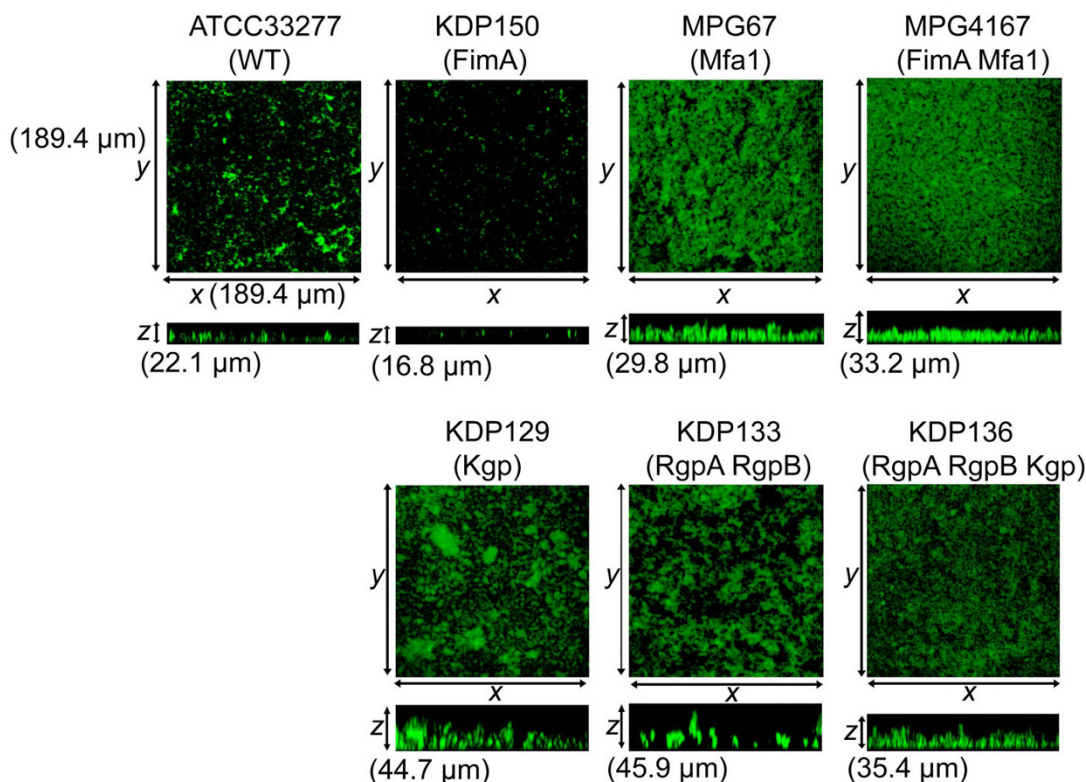


Figure 1

Homotypic biofilm formation by *P. gingivalis* wild-type strain and mutants in PBS. *P. gingivalis* strains were stained with CFSE (green) and incubated in PBS for 24 hours. After washing, the biofilms that developed on the coverglass were observed with a CLSM equipped with a 40 \times objective. Optical sections were obtained along the z axis at 0.7- μ m intervals, and images of the x-y and x-z planes were reconstructed with an imaging software as described in the text. Upper panels indicate z stacks of the x-y sections. Lower panels are x-z sections. *P. gingivalis* strains used in this assay are listed in Table 4. The experiment was repeated independently three times with each strain in triplicate. Representative images are shown.

cells in biofilms of each strain was tested by colony count and confirmed at 24 h (data not shown). These results suggest that the long fimbriae are involved in initial attachment and organization of biofilms by *P. gingivalis*, whereas the short fimbriae have a suppressive regulatory role for these steps.

The involvement of gingipains in biofilm formation was evaluated using a set of *P. gingivalis* mutants lacking Kgp (KDP129), RgpA/B (KDP133), or both Kgp and RgpA/B (KDP136). These mutants lacked the proteolytic domains as well as the adhesion domains of gingipains [5]. In addition, both Rgp mutants (KDP133 and KDP136) lacked bacterial cell-surface structural components such as long and short fimbriae and hemagglutinins which are processed by Rgp [21-23]. The Kgp mutant KDP129 formed markedly thick biofilms containing large accumulations of which the mean height was significantly taller than the wild type (Figure 1 and Table 1). In addition, the efficiency of autoaggregation in KDP129 was significantly increased (Table 2). These results suggest that Kgp plays a

negative role in biofilm development via suppressing autoaggregation and/or regulating dispersion, de-concentration, and/or detachment of microcolonies. The RgpA/B mutant KDP133 formed channel-like biofilms with fibrillar microcolonies (Figure 1), which featured significantly fewer peaks and longer distances between peaks, but increased height, as compared to those of the wild type and Kgp mutant (Table 1). Although the features of KDP133 were likely attributable to the loss of multiple factors on the bacterial surface, Rgp itself might be a bifunctional mediator promoting peak formation and shearing the fibrillar microcolonies of biofilms. Interestingly, the biofilms formed by the gingipain null mutant (KDP136) showed different features from both the Kgp (KDP129) and Rgp (KDP133) mutants. Although the three mutants, KDP136, KDP133 and MPG4167, resemble each other in terms of lack of expression of both types of fimbriae, their microstructures were divergent (Figure 1). These findings suggested that biofilm formation was affected not only by the post-translational regulation of the expression of cell surface components by Rgp, but also

Table 1: Features of biofilms formed by *P. gingivalis* wild-type strain and mutants in PBS

Strain	Peak parameters ^{a)}		
	Number of peaks	Mean distance between peaks (μm)	Mean peak height (μm)
ATCC33277 (wild type)	28.5 ± 3.3	3.0 ± 0.2	2.8 ± 0.4
KDP150 (Δ <i>fimA</i>)	14.7 ± 2.4**	5.4 ± 1.0**	2.7 ± 0.8
MPG67 (Δ <i>mfaI</i>)	29.3 ± 2.0	3.6 ± 0.2	16.6 ± 0.8**
MPG4167 (Δ <i>fimA</i> Δ <i>mfaI</i>)	30.5 ± 1.9	3.1 ± 0.2	12.7 ± 0.5**
KDP129 (Δ <i>kgp</i>)	25.5 ± 2.1	3.6 ± 0.3	12.7 ± 1.3**
KDP133 (Δ <i>rgpA</i> Δ <i>rgpB</i>)	13.0 ± 2.6**	8.4 ± 1.3**	23.2 ± 2.8**
KDP136 (Δ <i>rgpA</i> Δ <i>rgpB</i> Δ <i>kgp</i>)	30.5 ± 2.4	3.2 ± 0.2	12.7 ± 0.7**

^{a)} Number of peaks was evaluated in an area sized 90 (x axis) × 2 (y axis) μm. The mean ± SE of 10 areas was shown.

**p < 0.01 in comparison with the wild type using a Scheffe test.

by uncharacterized steps that were not altered by Rgp. Loss of all gingipain activities might result in downstream events which did not happen in KDP129 and KDP133.

Quantitative analysis of biofilms in PBS

The biovolume of the biofilms was also altered by deletion of various bacterial factors (Figure 2). The deletion of long fimbriae significantly reduced the biovolume, whereas the mutant without short fimbriae developed extensive biofilms. The deletion of Kgp also increased the biovolume, whereas no significant change was observed in the Rgp mutants. These results support the above sug-

gested roles; i.e., long fimbriae are a facilitator, short fimbriae and Kgp are suppressors, whereas Rgp has dual functions, promoting peak formation and shearing the fibrillar microcolonies, in the initial phase of biofilm formation by *P. gingivalis*.

Microstructure under proliferation condition

Next, the roles of the fimbriae and gingipains were examined in the early maturation phase of biofilms, which is associated with an increase in biovolume mainly due to cell division and exopolysaccharide accumulation. Biofilm development was induced by culture in nutrient medium. Figure 3 shows various features of biofilms of the mutants incubated in dTSB for 24 hours. The wild type strain formed biofilms with a dense basal monolayer with dispersed microcolonies, similar to the PBS condition, but with more and taller peaks (Table 3). The long fimbria mutant KDP150 formed biofilms with a thicker monolayer and with a greater number of the fine, taller peaks compared to wild type, (Figure 3 and Table 3). Those features suggested that long fimbriae have a role in suppression of the development of an thickened basal layer, but trigger protruding peak formation in early maturation phase. The short fimbria mutant MPG67 formed significantly clustered biofilms consisted of tall and wide microcolonies, suggesting that short fimbriae negatively control the morphology of microcolonies, as mentioned above. The mutant lacking both types of fimbriae (MPG4167) also formed markedly thick and dense biofilms containing various size of microcolonies, suggesting that both types of fimbriae negatively regulate biofilm formation in early maturation phase. The Kgp mutant KDP129 formed large microcolonies which were well dispersed, whereas the Rgp mutant KDP133 made the most thick biofilms with the tallest acicular microcolonies (Figure 3 and Table

Table 2: Autoaggregation of *P. gingivalis* wild-type strain and mutants

Strain	Autoaggregation index ^{a)} (-dA/min)
ATCC33277 (wild type)	17.73 ± 1.67
KDP150 (Δ <i>fimA</i>)	0.54 ± 3.94**
MPG67 (Δ <i>mfaI</i>)	36.12 ± 2.40**
MPG4167 (Δ <i>fimA</i> Δ <i>mfaI</i>)	33.87 ± 2.77**
KDP129 (Δ <i>kgp</i>)	35.62 ± 2.52**
KDP133 (Δ <i>rgpA</i> Δ <i>rgpB</i>)	15.04 ± 2.68
KDP136 (Δ <i>rgpA</i> Δ <i>rgpB</i> Δ <i>kgp</i>)	0.29 ± 3.22**

^{a)} dA/min was automatically calculated by subtraction of At, the absorbance at time t min, from At+, at time (t + 1) min during incubation. The maximum value of -dA/min in a curve was used as the autoaggregation index. The data represent the mean ± SE of three separate experiments with each strain in duplicate.

**p < 0.01 in comparison with the wild type using a Scheffe test.

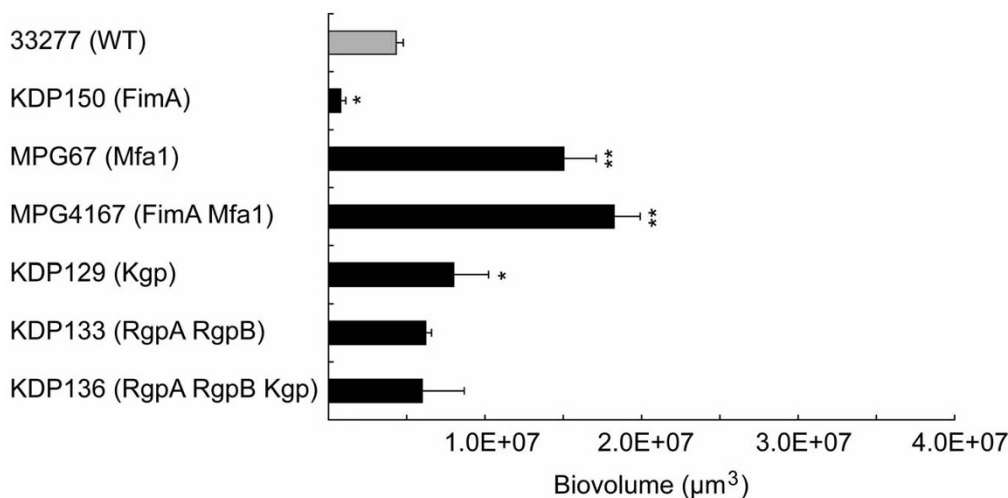


Figure 2
Quantification of homotypic biofilms formed by *P. gingivalis* wild-type strain and mutants in PBS. Biofilms were formed as described in Figure 1, and 10 fields per a sample were randomly recorded and quantified with a CLSM. Z stacks of the x-y sections were converted to composite images to quantify each biovolume as described in the text. Standard error bars are shown. Statistical analysis was performed using a Scheffe test. **p* < 0.05 and ***p* < 0.01 in comparison to the wild-type strain. *P. gingivalis* strains used in this assay are listed in Table 4.

3). These findings suggested that Kgp suppresses micro-colony expansion, whereas Rgp mediates transverse enlargement and restrains the longitudinal extension. As with the result in PBS, biofilms with the gingipain null mutant KDP136 showed different features from both KDP129 and KDP133.

Quantitative analysis of biofilms in dTSB

In the early maturation phase, the biovolumes of the biofilms were significantly increased in all of tested mutants as compared to the wild type (Figure 4). Deletion of long fimbriae resulted in the opposite tendency from the initial

attachment phase, suggesting that this molecule has distinct roles under the different phases.

Exopolysaccharide production under proliferation conditions

As extracellular polysaccharide is important for the development of biofilm communities, we examined the influences of fimbriae and gingipains on the accumulation of exopolysaccharide in *P. gingivalis* biofilms. To visualize and quantify exopolysaccharide accumulation in biofilms under the proliferation condition, 4',6-diamino-2-phenylindole (DAPI)-labeled *P. gingivalis* cells and fluores-

Table 3: Features of biofilms formed by *P. gingivalis* wild-type strain and mutants in dTSB

Strain	Peak parameters ^{a)}		
	Number of peaks	Mean distance between peaks (µm)	Mean peak height (µm)
ATCC33277 (wild type)	45.5 ± 3.5	2.0 ± 0.9	6.9 ± 1.4
KDP150 ($\Delta fimA$)	52.5 ± 3.5*	1.7 ± 0.7*	23.7 ± 5.6**
MPG67 ($\Delta mfa1$)	35.8 ± 3.6**	2.7 ± 1.6**	20.9 ± 4.4**
MPG4167 ($\Delta fimA\Delta mfa1$)	32.3 ± 3.8**	3.0 ± 1.6**	20.5 ± 4.3**
KDP129 (Δkgp)	39.8 ± 3.2	2.2 ± 1.2	19.6 ± 5.4**
KDP133 ($\Delta rgpA\Delta rgpB$)	41.0 ± 5.7	2.2 ± 1.0	45.9 ± 4.5**
KDP136 ($\Delta rgpA\Delta rgpB\Delta kgp$)	43.0 ± 1.4	2.1 ± 0.8	22.2 ± 2.4**

^{a)}Number of peaks was evaluated in an area sized 90 (x axis) × 2 (y axis) µm. The mean ± SE of 10 areas was shown. **p* < 0.05 and ***p* < 0.01 in comparison with the wild type using a Scheffe test.

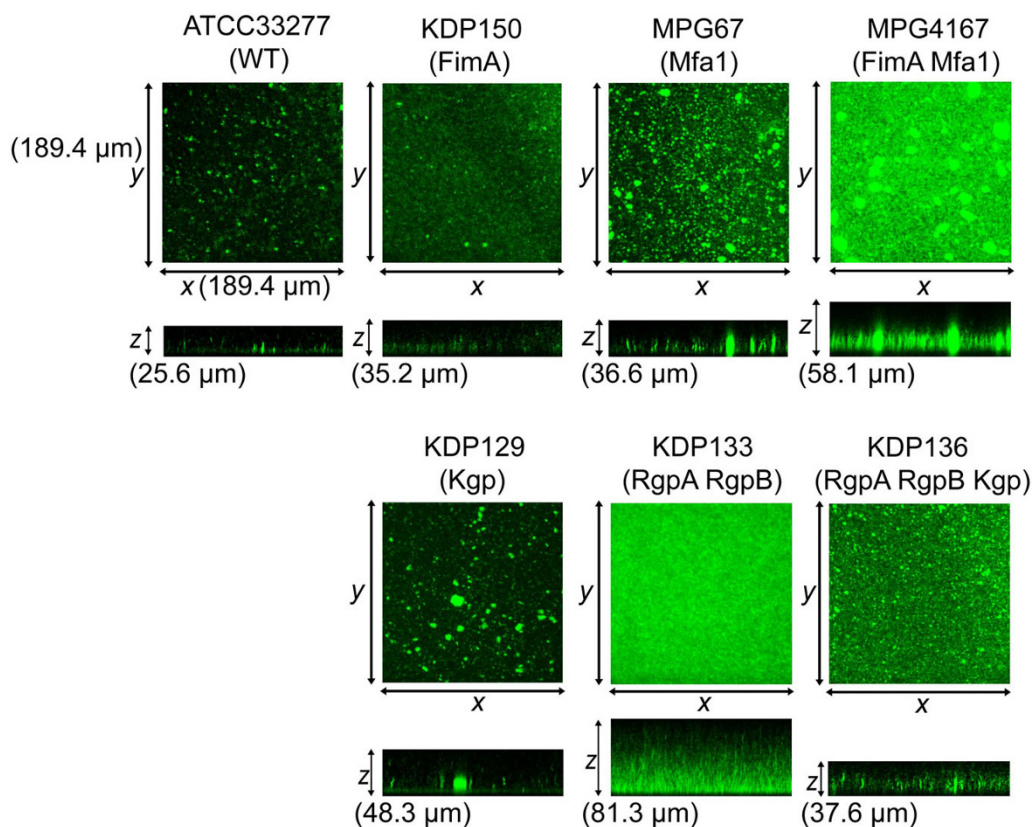


Figure 3

Homotypic biofilm formation by *P. gingivalis* wild-type strain and mutants in dTSB. *P. gingivalis* strains were stained with CFSE (green) and incubated in dTSB for 24 hours. After washing, the biofilms that developed on the coverglasses were observed with a CLSM equipped with a 40 \times objective. Optical sections were obtained along the z axis at 0.7- μ m intervals, and images of the x-y and x-z planes were reconstructed with imaging software, as described in the text. Upper panels indicate z stacks of the x-y sections. Lower panels show x-z sections. The experiment was repeated independently three times with each strain in triplicate. Representative images are shown.

cein isothiocyanate (FITC)-labeled exopolysaccharide were examined by confocal microscopy with digitally reconstructed image analysis. In all of the tested strains, DAPI-labeled cells exhibited the same microstructures of biofilms composed of 5-(and-6)-carboxyfluorescein succinimidyl ester (CFSE)-labeled cells, as shown in Figure 3, thus validating the use of these live-staining methods (data not shown). Exopolysaccharide visualization enabled us to assess the accumulation pattern (Figure 5A) and exopolysaccharide biovolume per base area (Figure 5B). Furthermore, the exopolysaccharide production was normalized to the levels of DAPI-labeled *P. gingivalis* cells in the biofilms and expressed as the exopolysaccharide/cell ratio (Figure 5C). Interestingly, a unique pattern of exopolysaccharide accumulation was observed in the Rgp mutant KDP133 in vertical sections (x-z plane) of biofilms (Figure 5A). In contrast to the other strains, exopolysaccharide accumulated in the middle layer, and the biofilm surface was not covered with exopolysaccharide. It was also notable that the long fimbria mutant KDP150 devel-

oped a biofilm enriched with exopolysaccharide (Figure 5A), reflecting a significantly higher exopolysaccharide/cell ratio (Figure 5C). The gingipain null mutant KDP136 produced the most abundant exopolysaccharide per unit base area (Figure 5B). The minor fimbria mutant MPG67, long/short fimbriae mutant MPG4167 and Rgp mutant KDP133 also accumulated significantly larger amounts of exopolysaccharide than wild type; however, exopolysaccharide/cell ratio in KDP133 and MPG4167 was significantly lower than wild type because biofilms of these strains consisted of larger numbers of cells (Figure 5C).

Autoaggregation

Bacterial autoaggregation has been reported to play an important role in initial biofilm formation [24], thus the autoaggregation efficiencies of the mutants were assessed (Table 2). Deletion of long fimbriae significantly reduced the autoaggregation efficiency, which agreed with the previous report that long fimbriae were required for autoaggregation [25]. The efficiency of autoaggregation was

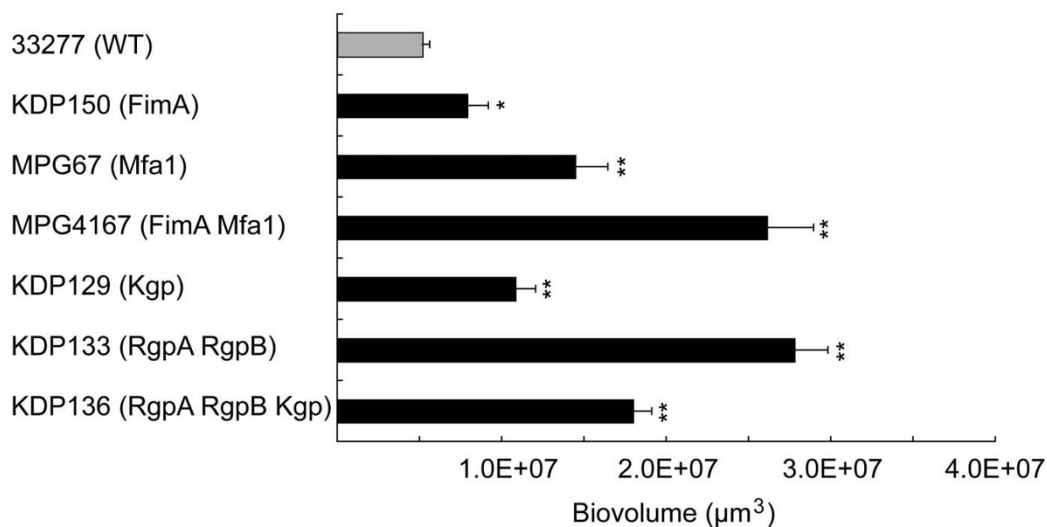


Figure 4

Quantification of homotypic biofilms formed by *P. gingivalis* wild-type strain and mutants in dTSB. Biofilms were formed as described in the legend to Figure 3, and 10 fields per a sample were randomly recorded and quantified, similar to the method described in the legend to Figure 2. Statistical analysis was performed with a Scheffe test. * $p < 0.05$ and ** $p < 0.01$ in comparison to the wild-type strain.

significantly increased in the Kgp mutant KDP129, short fimbria mutant MPG67 and long/short fimbriae deficient mutant MPG4167, suggesting that Kgp and short fimbriae act to suppress autoaggregation. Contrary to our prediction, the gingipain null mutant KDP136 and Rgp mutant KDP133 showed different tendencies of autoaggregation from MPG4167, although all of these strains were considered to be long/short fimbriae deficient mutants. Thus, not only fimbrial expression but also other factors, modified by gingipains, seem to be involved in autoaggregation. In addition, it was found that autoaggregation and biofilm parameters such as biovolume, number of peaks and peak height were not significantly correlated in every strain (Figure 2, Figure 4, Table 1 and Table 3). This result suggests that autoaggregation is not the sole determinant of alteration in structure of *P. gingivalis* biofilms.

Tenacity of biofilms

To analyze the influence of the molecules under investigation on vulnerability of biofilms, the physical strength of the biofilms against brief ultrasonication was compared (Figure 6). Consistent with the results of image analysis described in Figure 4 and Figure 5A, the long/short fimbriae mutant MPG4167 and Rgp mutant KDP133 formed expansive biofilms with large numbers of cells in dTSB, however, their strength was found to be very fragile compared to the other strains, suggesting that these biofilms consisted of loosely connected microcolonies. In contrast, the biofilms of the long fimbria mutant KDP150 were resistant to sonic disruption, suggesting that long fimbriae are initial mediator of biofilm formation but are not

required to maintain resistance against environmental shear force.

Collectively, these results suggest that long fimbriae are required for initial formation of biofilms by *P. gingivalis*, but suppress the development of an exopolysaccharide-enriched basal layer that is related to the adhesive property of biofilms. In contrast, short fimbriae and Kgp may have suppressive and regulatory roles for biofilm formation, with control over morphology of microcolonies, whereas Rgp mediates microcolony formation and restrains the biovolume. In addition, other factors beside fimbriae and gingipains are likely involved in homotypic biofilm formation by *P. gingivalis*.

Discussion

Dental plaque, a precursor for periodontal disease, is also a well studied model of bacterial biofilms in general [26,27]. Developing biofilm communities in the oral cavity are fundamental for the persistence of organisms such as *P. gingivalis* and continual exposure of the host to *P. gingivalis* can result in a dysfunctional immune response [28]. Biofilm maturation proceeds through a series of developmental steps involving the attachment of cells to, and growth on, a surface, followed by detachment and dissemination to a new site to start the cycle again [29,30]. It is likely that much of biofilm-specific physiology is devoted to dynamic changes that both stimulate an increase in biovolume and limit or stabilize accumulation according to environmental constraints. Therefore, multiple bacterial factors are thought to be required to regulate appropriate biofilm structure.

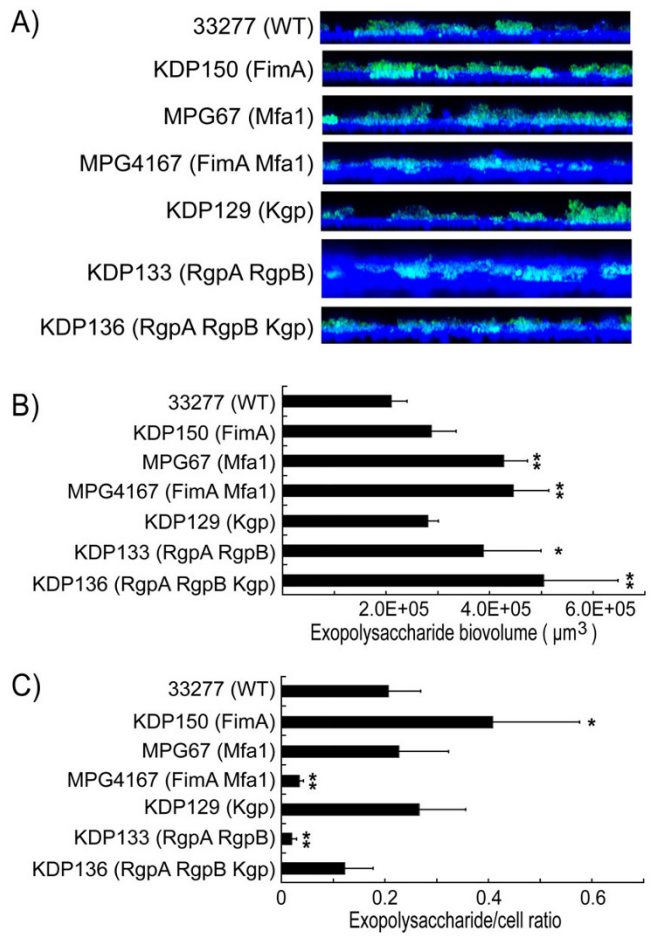


Figure 5
Exopolysaccharide production by *P. gingivalis* wild-type strain and mutants in dTSB. A) Visualization of exopolysaccharide production in biofilms formed by *P. gingivalis* strains after staining with FITC-labelled concanavalin A and wheat germ agglutinin (green). Bacteria were stained with DAPI (blue). Fluorescent images were obtained using a CLSM. The z stack of the x-y sections was converted to composite images with the "Volume" function using Imaris software, after which a y stack of the x-z sections was created and is presented here. B) Fluorescent images were quantified using Imaris software and average of total exopolysaccharide biovolume per field was calculated. C) Exopolysaccharide levels are expressed as the ratio of exopolysaccharide/cells (FITC/DAPI) fluorescence. The experiment was repeated independently three times. Data are presented as averages of 8 fields per sample with standard errors of the means. Statistical analysis was performed using a Scheffe test. **p* < 0.05 and ***p* < 0.01 in comparison to the wild-type strain.

mentioned dynamic changes that stimulate, limit or stabilize the biofilm formation. Long fimbriae were shown to be initial positive mediators of biofilm formation, however, these appendages also functioned to decrease the adhesive property of biofilms via repressing exopolysaccharide accumulation in basal layer. In addition, short fimbriae as well as Kgp were found to be negative regulators of microcolony formation and of biovolume. Rgp seems to play a bifunctional role in coordinating the integrity of the biofilm through mediating microcolony formation and restraining the biovolume. Our results indicate that all of these interactions are likely to be coordinately essential for the initiation and development of appropriately structured biofilms. To our knowledge, this is the first report to evaluate the roles of long/short fimbriae as well as gingipains on *P. gingivalis* biofilm formation.

Interestingly, the distinct fimbria types functioned differently in regard to biofilm formation. Our findings agree with a recent report [17], which suggested that long fimbriae are required for initial attachment and organization of biofilms. In that study, it was also shown that short fimbriae promoted bacterial autoaggregation, whereas long fimbriae suppressed it. Other studies have shown that autoaggregation is attributable to long fimbriae on the cell surface [18,31,32], and deletion of short fimbriae enhances autoaggregation [18], more consistent with our present findings. However, it would appear that autoaggregation is context and assay dependent, and in any event not a good predictor of accumulation on abiotic surfaces.

Recently, it was reported that ClpXP, a proteolytic core and associated ATPase unit of the bacterial stress response system, negatively regulated the surface exposure of short fimbriae, and a ClpXP mutant showed elevated monospecies biofilm formation [33]. As we have shown here that the short fimbria mutant MPG67 developed greater biofilm accumulation than the wild type, it is likely that ClpXP has numerous effects on cell surface molecules important in biofilm development.

The long/short fimbriae mutant MPG4167 and RgpA/B mutant KDP133 developed biofilms with significantly large amounts of bacterial cells. In addition, the exopolysaccharide/cell ratio was significantly smaller than the other strains, and the biofilms of these strains were shown to be fragile (Figures 5C and 6). Rgp is an enzyme that processes precursor proteins of bacterial surface components such as fimbriae [22,23], therefore, Rgp-null mutants exhibit defective surface protein presentation. Thus not only MPG4167 but also KDP133 do not have intact fimbrial protein on the cell surface, which might be related to imperfect anchoring of exopolysaccharide on the bacterial surfaces. The gingipains null mutant KDP136 did not show the same tendency in spite of the lack of

In the present study, the roles of long/short fimbriae and gingipains on the initiation and development of biofilms formed by *P. gingivalis* were examined. Interestingly, those molecules were found to play distinct roles in the above-

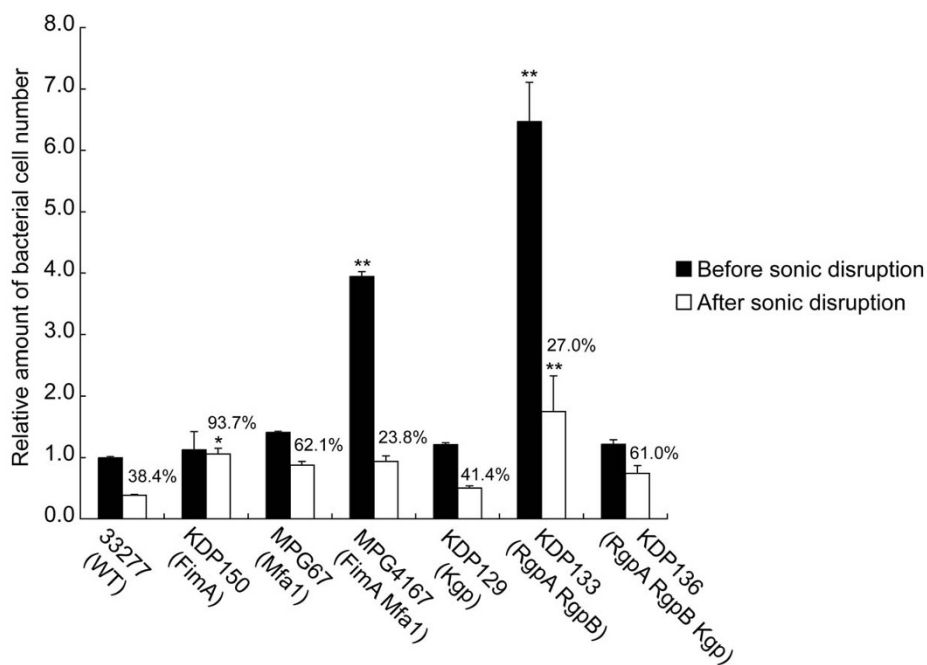


Figure 6

Tenacity of biofilms formed by *P. gingivalis* wild tstrain and mutants. Standardized cultures of *P. gingivalis* were inoculated into dTSB in saliva-coated 12-well polystyrene plate and incubated in a static manner at 37°C for 60 hours, with the resulting biofilms sonicated for 1 second. Immediately after sonication, supernatants containing floating cells were removed by aspiration and the biofilm remains were gently washed with PBS. *P. gingivalis* genomic DNA was isolated from the biofilms and the numbers of *P. gingivalis* cells were determined using real-time PCR. Relative amounts of bacterial cell numbers were calculated based on the number of wild-type cells without sonication considered to be 1.0. Percentages shown indicate the amount of remaining biofilm after sonic disruption. The experiment was repeated independently three times with each strain in duplicate. Standard error bars are shown. Statistical analysis was performed using a Scheffe test. * $p < 0.05$ and ** $p < 0.01$ in comparison to the wild-type strain.

both types of fimbriae, suggesting the presence of Kgp was related to the unusual exopolysaccharide accumulation. In contrast, long fimbriae mutant KDP150 formed a tough and cohesive biofilm, and its exopolysaccharide/cell ratio was significantly higher than the other strains. Together, these findings suggest that the exopolysaccharide/cell ratio seems to be related to the physical strength of *P. gingivalis* biofilms.

The specific role of Kgp may involve regulation of biofilm formation by the dispersion, de-concentration, and/or detachment of microcolonies. Rgp also seemed to coordinate the integrity of the biofilm in the developing phase as well as maturation phase. There are several reports which suggest that the present morphological changes in proteinase mutants were possibly due to loss of proteolytic activities. In *Staphylococcus aureus*, increased levels of serine proteases were detected in detaching biofilm effluents, and a serine protease inhibitor suppressed the biofilm detachment [34]. In the same report, a double mutant in a metalloprotease and serine proteases, which displayed minimal extracellular pro-

tease activity, showed significantly enhanced biofilm formation and a strongly attenuated detachment phenotype. In *Streptococcus pneumoniae*, trypsin or proteinase K was shown to inhibit biofilm development, and incubation of mature biofilms with proteinase K drastically diminished the number of biofilm-associated sessile cells [35]. Since our data also showed that the mutation in gingipain genes resulted in enhanced biofilm formation as well as a strongly attenuated detachment phenotype, this suggests that proteinase domains of Kgp and Rgp are significantly involved in biofilm regulation [5]. In addition, the tyrosine phosphatase Ltp1 reportedly dephosphorylated gingipains, resulting in suppression of biofilm formation [10], which also supports the involvement of gingipains as shown in this study. Furthermore, the present gingipain mutants lacked proteinase domains as well as C-terminal flanking segments coding for hemagglutinin/adhesin (HA) domains [36]. Higher concentrations of iron in the cultivation media can have a positive effect on the stability of the biofilms [37], thus decreased hemin uptake due to the lack of HA domains might modulate the biofilm structures in dTSB.

Table 4: *P. gingivalis* strains used in this study

Strain	Genotype	Relevant properties	Reference
33277	Wild type	Wild type	ATCC
KDP150	<i>fimA::erm</i>	Long fimbria (FimA)- deficient	[20]
MPG67	<i>mfal::erm</i>	Short fimbria (MfaI)- deficient	[18]
MPG4167	<i>fimA::erm mfal::tetQ</i>	Long and short fimbria-deficient	[18]
KDP129	<i>kgp::cat</i>	Kgp-null	[20]
KDP133	<i>rgpA::tetQ rgpB::erm</i>	Rgp-null	[20]
KDP136	<i>rgpA::erm rgpB::tetQ kgp::cat</i>	Rgp/Kgp-null	[20]

Autoaggregation driven by nonspecific hydrophobic mechanisms is thought to contribute to hetero- and homo-typic biofilm formation [24]. Indeed, the significant change of autoaggregation efficiencies in KDP129, KDP150, MPG67 and MPG4167 were found to be positively associated with alteration of biofilm structures under the non-proliferation condition. However, such an association was not observed in Rgp-null mutant strains, KDP133 and KDP136, and was not significant under the proliferation condition. Our present results suggested that a biofilm-regulatory molecule Rgp does not function through autoaggregation but rather through other mechanisms mediating intimate contact among *P. gingivalis* cells. Recently Kato *et al.* found that autoaggregation ability correlated poorly with the hydrophobicity in FimA-substituted mutants [38]. In addition, the hydrophobicity was reported not to depend on the presence or absence of FimA on the bacterial surface [39]. In-depth mathematical and physical examinations may be needed to explain the complicated roles of hydrophobicity, autoaggregation and cell surface structure on biofilm development.

Besides fimbria and proteinases, our findings indicate that other molecules of *P. gingivalis*, which are not processed by gingipains, mediate homotypic biofilm formation. Indeed several factors, including a putative glycosyltransferase (PG_0106), UDP-galactose 4-epimerase (GalE), internalin J protein (InlJ), a universal stress protein (UpsA), and a low molecular weight tyrosine phosphatase (Ltp1), have been reported to be required for homotypic biofilm formation by *P. gingivalis* [10,19,40-42]. Autoinducer-2, which regulates proteinase and hemagglutinin activities, hemin and iron acquisition pathways, and stress gene expression, is also considered to be involved in homotypic biofilm formation [43-46]. It is possible that these molecules also have effects in regard to biofilm structure alterations, in addition to fimbriae and gingipains. Further work is necessary to understand the complete process of the biofilm formation by *P. gingivalis*.

Conclusion

The present results suggest distinct roles of long/short fimbriae and gingipains in homotypic biofilm development

by *P. gingivalis*. Long fimbriae are initial positive mediators of biofilm formation, and thereafter they decrease the expression of exopolysaccharide to regulate adhesive properties. Short fimbriae as well as Kgp are negative regulators of microcolony formation. Rgp plays a bifunctional role to coordinate the integrity of the biofilm through mediating microcolony formation and restraining biovolume. Collectively, these molecules seem to act coordinately to regulate the development of mature biofilms.

Methods

Bacterial strains and media

The *P. gingivalis* strains used in this study are shown in Table 4. *P. gingivalis* cells were inoculated from blood agar plates and grown anaerobically (85% N₂, 10% H₂, 5% CO₂) at 37°C in trypticase soy broth supplemented with 1 mg/ml of yeast extract, 1 µg/ml of menadione and 5 µg/ml of hemin (TSB). At stationary phase, the cells were harvested by centrifugation at 6,000 × g for 7 minutes, resuspended in pre-reduced 10 mM phosphate buffer containing 0.15 M sodium chloride (PBS; pH 7.4) and then used in the assays. When necessary, the following antibiotics were used at the concentrations shown in parentheses: chloramphenicol (20 µg/ml), erythromycin (10 µg/ml), and tetracycline (1 µg/ml). To observe initial attachment and organization of biofilms, *P. gingivalis* cells were anaerobically incubated in pre-reduced PBS without a nutrition source [19]. In order to monitor an increase in biovolume due to cell division as well as exopolysaccharide accumulation, bacterial cells were cultured in TSB medium diluted with PBS (dTSB; TSB/PBS ratio, 1:2) [47].

Autoaggregation assay

An autoaggregation assay was essentially performed as described previously [48]. Briefly, 1 ml of *P. gingivalis* suspension (4 × 10⁸ cells) was transferred into a UV-cuvette then incubated at 37°C with stirring. Autoaggregation was monitored by measuring the decrease in optical density at A₅₅₀ (OD₅₅₀) using a UV-visible recording spectrophotometer (UV-265FW; Shimadzu Co. Kyoto, Japan). During the incubation, dA/dt was continuously calculated and recorded by subtraction of At, the absorbance at time

t min, from At+, at time (t + 1) min. The maximum value of $-dA/dt$ in this curve was used as the autoaggregation activity [48]. The data represent the mean \pm standard error of three separate experiments with each strain in duplicate.

Saliva

Saliva stimulated by mastication of paraffin balls was collected in a sterile centrifuge tube on ice from healthy donors and pooled, as described previously [49]. Dithiothreitol (Sigma-Aldrich, St. Louis, MO) was added to a 2.5 mM final concentration, then the saliva was gently stirred on ice for 10 minutes and centrifuged at $3,000 \times g$ for 20 minutes at 4°C. The clarified saliva supernatant was decanted, 3 volumes of distilled water was added, and the 25% saliva was filtered through a 0.20 μm pore size filter and frozen in 40 ml aliquots. Immediately prior to use, the sterile saliva was thawed at 37°C; the slight precipitate was pelleted at $1,430 \times g$ for 5 min, and the clear 25% saliva supernatant was used in experiments.

Microscope observation

Quantitative and structural analysis of homotypic *P. gingivalis* biofilms was accomplished by confocal laser scanning microscopy (CLSM, Radiance 2100, Bio-Rad) and subsequent image analysis [50]. *P. gingivalis* was stained with CFSE (8 $\mu\text{g}/\text{ml}$; Molecular Probes, Eugene, OR), washed three times and 1×10^8 cells in PBS or dTSB were anaerobically incubated in a 25% saliva-coated wells of a chambered coverglass system (Culture Well™, Grace Bio Labs, Bend, OR) for 24 hours at 37°C in the dark on a rotator. The resulting biofilms were examined using the CLSM with reflected laser light at 488 nm. The images were analyzed using the Image J 1.34s (National Institutes of Health; Bethesda, MD) and Imaris 5.0.1 (Bitplane AG; Zurich, Switzerland) software packages. The experiment was repeated independently three times with each strain in triplicate.

Biofilm characterization by image analysis

Z stacks of the *x-y* sections in the CLSM images were converted to composite images with the "Iso Surface" function of the "Surpass" option provided by Imaris 5.0.1 (Bitplane AG; Zurich, Switzerland) software. Iso Surface images were created at a threshold of 40 and smoothed with the "Gaussian Filter" function at a width of 1.28 μm , then the biovolume was calculated. Measurement of peak parameters was performed as described previously [50]. Digitally reconstructed images of the *x-z* section, 189.4 $\mu\text{m} \times$ appropriate height with 10- μm spaced γ -series slices, were created using the "Reslice" function of Image J. An image series of the *x-z* section was processed using the "Find Edges" function, then the peak height was calculated by Image J. Color images of the *x-z* section were converted into gray scale and the density per vertical position (*x*-axis) was analyzed with the "Plot profile" function of

Image J. The data were then exported as plot values with *x*-axis distance information. Peaks were defined as positions where plot values were higher than on either side, and the distance between two peaks was measured. The peak number was counted in a 90- μm section of the *x*-axis.

Exopolysaccharide production assay

P. gingivalis organisms were stained with DAPI (50 $\mu\text{g}/\text{ml}$; Molecular Probes, Eugene, OR), then washed and cultured in 25% saliva-coated wells of CultureWell chambered coverglass system with dTSB for 24 hours. The resulting biofilms were washed, then exopolysaccharide was labelled with Concanavalin A-FITC and Wheat germ agglutinin-FITC (100 $\mu\text{g}/\text{ml}$; Molecular Probes) for 30 minutes at room temperature, as described previously [10]. After washing, fluorescent images were obtained using CLSM with reflected laser light at 405 and 488 nm, then analyzed as described above. The images were obtained with 8 fields per a sample. The experiment was repeated independently three times.

Sonic disruption assay

A 12-well polystyrene plate (#1820-024, AGC Techno Glass, Chiba, Japan) was coated with 25% saliva. *P. gingivalis* cells (4×10^8 cfu/well) were incubated in a static manner in dTSB for 60 hours at 37°C and the resulting biofilms were sonicated for 1 second at output level 1 (output power: 25 W, oscillating frequency: 28 kHz, tip diameter: 2.5 mm) with a Handy ultrasonic disruptor (UR-20P, Tomy Seiko, Tokyo, Japan). During sonication, the oscillator was fixed with a stand, and the tip of horn was positioned 5 mm above from the center point of flat well bottoms. Immediately after the sonication, supernatants containing floating cells were removed by aspiration and the remaining biofilms were gently washed with PBS. *P. gingivalis* genomic DNA was isolated from the biofilms and the number of *P. gingivalis* cells per well was determined using real-time PCR, as described previously [51]. The data represent the means \pm standard error of three separate experiments with each strain in duplicate.

Statistical analyses

All data are expressed as the mean \pm standard error. Multiple comparisons were performed by one-way analysis of variance and Sheffe's test using the SPSS 16.0J software (SPSS Japan Inc., Tokyo).

Abbreviations

TSB: trypticase soy broth supplemented with 1 mg/ml of yeast extract, 1 $\mu\text{g}/\text{ml}$ of menadione and 5 $\mu\text{g}/\text{ml}$ of hemin; DAPI: 4',6-diamino-2-phenylindole; FITC: fluorescein isothiocyanate; CFSE: 5-(and-6)-carboxyfluorescein succinimidyl ester; CLSM: confocal laser scanning microscopy; dTSB: diluted TSB medium.

Authors' contributions

MK carried out the microscope observation, image analysis and autoaggregation assay, as well as prepared the initial draft of the manuscript. AA conceived of the study and helped to draft the manuscript. EH and YY carried out the sonic disruption assay. HI performed the statistical analysis. KN and NH provided *P. gingivalis* knockout mutants used in this study. GDT developed the exopolysaccharide assay for *P. gingivalis*. RJL participated in the design of the study and helped to draft the manuscript. SS participated in the design of the study and coordination. All authors read and approved the final manuscript.

Acknowledgements

This research was supported in part by a grant from the 21st Century Center of Excellence program entitled "Origination of Frontier BioDentistry" held at Osaka University Graduate School of Dentistry, as well as grants-in-aid for Scientific Research on Priority Areas and grants-in-aid for Scientific Research from the Ministry of Education, Culture, Sports, Science and Technology, and DE12505 from the NIH

References

- Lamont RJ, Jenkinson HF: **Life below the gum line: pathogenic mechanisms of *Porphyromonas gingivalis*.** *Microbiol Mol Biol Rev* 1998, **62**:1244-1263.
- Holt SC, Ebersole JL: ***Porphyromonas gingivalis*, *Treponema denticola*, and *Tannerella forsythia*: the "red complex", a prototype polybacterial pathogenic consortium in periodontitis.** *Periodontol 2000* 2005, **38**:72-122.
- Imamura T: **The role of gingipains in the pathogenesis of periodontal disease.** *J Periodontol* 2003, **74**:111-118.
- Paramonov N, Rangarajan M, Hashim A, Gallagher A, Aduse-Opoku J, Slaney JM, Hounsell E, Curtis MA: **Structural analysis of a novel anionic polysaccharide from *Porphyromonas gingivalis* strain W50 related to Arg-gingipain glycans.** *Mol Microbiol* 2005, **58**:847-863.
- Kadowaki T, Nakayama K, Okamoto K, Abe N, Baba A, Shi Y, Ratnayake DB, Yamamoto K: ***Porphyromonas gingivalis* proteinases as virulence determinants in progression of periodontal diseases.** *J Biochem* 2000, **128**:153-159.
- Chen T, Duncan MJ: **Gingipain adhesin domains mediate *Porphyromonas gingivalis* adherence to epithelial cells.** *Microb Pathog* 2004, **36**:205-209.
- Labrecque J, Bodet C, Chandad F, Grenier D: **Effects of a high-molecular-weight cranberry fraction on growth, biofilm formation and adherence of *Porphyromonas gingivalis*.** *J Antimicrob Chemother* 2006, **58**:439-443.
- Yamanaka A, Kouchi T, Kasai K, Kato T, Ishihara K, Okuda K: **Inhibitory effect of cranberry polyphenol on biofilm formation and cysteine proteases of *Porphyromonas gingivalis*.** *J Periodontol Res* 2007, **42**:589-592.
- Yamada M, Ikegami A, Kuramitsu HK: **Synergistic biofilm formation by *Treponema denticola* and *Porphyromonas gingivalis*.** *FEMS Microbiol Lett* 2005, **250**:271-277.
- Maeda K, Tribble GD, Tucker CM, Anaya C, Shizukuishi S, Lewis JP, Demuth DR, Lamont RJ: **A *Porphyromonas gingivalis* tyrosine phosphatase is a multifunctional regulator of virulence attributes.** *Mol Microbiol* 2008, **69**:1153-1164.
- Amano A, Nakagawa I, Okahashi N, Hamada N: **Variations of *Porphyromonas gingivalis* fimbriae in relation to microbial pathogenesis.** *J Periodontol Res* 2004, **39**:136-142.
- Hajishengallis G, Harokopakis E: ***Porphyromonas gingivalis* interactions with complement receptor 3 (CR3): innate immunity or immune evasion?** *Front Biosci* 2007, **12**:4547-4557.
- Hajishengallis G, Wang M, Liang S, Triantafilou M, Triantafilou K: **Pathogen induction of CXCR4/TLR2 cross-talk impairs host defense function.** *Proc Natl Acad Sci USA* 2008, **105**:13532-13537.
- Amano A: **Disruption of epithelial barrier and impairment of cellular function by *Porphyromonas gingivalis*.** *Front Biosci* 2007, **12**:3965-3974.
- Kuboniwa M, Hasegawa Y, Mao S, Shizukuishi S, Amano A, Lamont RJ, Yilmaz O: ***P. gingivalis* accelerates gingival epithelial cell progression through the cell cycle.** *Microbes Infect* 2008, **10**:122-128.
- Park Y, Simonato MR, Sekiya K, Murakami Y, James D, Chen W, Hackett M, Yoshimura F, Demuth DR, Lamont RJ: **Short fimbriae of *Porphyromonas gingivalis* and their role in coadhesion with *Streptococcus gordonii*.** *Infect Immun* 2005, **73**:3983-3989.
- Lin X, Wu J, Xie H: ***Porphyromonas gingivalis* minor fimbriae are required for cell-cell interactions.** *Infect Immun* 2006, **74**:6011-6015.
- Umamoto T, Hamada N: **Characterization of biologically active cell surface components of a periodontal pathogen. The roles of major and minor fimbriae of *Porphyromonas gingivalis*.** *J Periodontol* 2003, **74**:119-122.
- Capestany CA, Kuboniwa M, Jung IY, Park Y, Tribble GD, Lamont RJ: **Role of the *Porphyromonas gingivalis* InI protein in homotypic and heterotypic biofilm development.** *Infect Immun* 2006, **74**:3002-3005.
- Shi Y, Ratnayake DB, Okamoto K, Abe N, Yamamoto K, Nakayama K: **Genetic analyses of proteolysis, hemoglobin binding, and hemagglutination of *Porphyromonas gingivalis*. Construction of mutants with a combination of *rgpA*, *rgpB*, *kgp*, and *hagA*.** *J Biol Chem* 1999, **274**:17955-17960.
- Kadowaki T, Nakayama K, Yoshimura F, Okamoto K, Abe N, Yamamoto K: **Arg-gingipain acts as a major processing enzyme for various cell surface proteins in *Porphyromonas gingivalis*.** *J Biol Chem* 1998, **273**:29072-29076.
- Nakayama K, Yoshimura F, Kadowaki T, Yamamoto K: **Involvement of arginine-specific cysteine proteinase (Arg-gingipain) in fimbriation of *Porphyromonas gingivalis*.** *J Bacteriol* 1996, **178**:2818-2824.
- Shoji M, Naito M, Yukitake H, Sato K, Sakai E, Ohara N, Nakayama K: **The major structural components of two cell surface filaments of *Porphyromonas gingivalis* are matured through lipoprotein precursors.** *Mol Microbiol* 2004, **52**:1513-1525.
- Kolenbrander PE, Palmer RJ Jr, Rickard AH, Jakubovics NS, Chalmers NI, Diaz PI: **Bacterial interactions and successions during plaque development.** *Periodontol 2000* 2006, **42**:47-79.
- Kato T, Tsuda T, Omori H, Kato T, Yoshimori T, Amano A: **Maturation of fimbria precursor protein by exogenous gingipains in *Porphyromonas gingivalis* gingipain-null mutant.** *FEMS Microbiol Lett* 2007, **273**:96-102.
- Jenkinson HF, Lamont RJ: **Oral microbial communities in sickness and in health.** *Trends Microbiol* 2005, **13**:589-595.
- Kuramitsu HK, He X, Lux R, Anderson MH, Shi W: **Interspecies interactions within oral microbial communities.** *Microbiol Mol Biol Rev* 2007, **71**:653-670.
- Lamont RJ, Jenkinson HF: **Subgingival colonization by *Porphyromonas gingivalis*.** *Oral Microbiol Immunol* 2000, **15**:341-349.
- O'Toole GA: **Microbiology: Jekyll or hide?** *Nature* 2004, **432**:680-681.
- Stoodley P, Sauer K, Davies DG, Costerton JW: **Biofilms as complex differentiated communities.** *Annu Rev Microbiol* 2002, **56**:187-209.
- Andrian E, Grenier D, Rouabhia M: ***Porphyromonas gingivalis*-epithelial cell interactions in periodontitis.** *J Dent Res* 2006, **85**:392-403.
- Kuramitsu H, Tokuda M, Yoneda M, Duncan M, Cho MI: **Multiple colonization defects in a cysteine protease mutant of *Porphyromonas gingivalis*.** *J Periodontol Res* 1997, **32**:140-142.
- Capestany CA, Tribble GD, Maeda K, Demuth DR, Lamont RJ: **Role of the Clp system in stress tolerance, biofilm formation, and intracellular invasion in *Porphyromonas gingivalis*.** *J Bacteriol* 2008, **190**:1436-1446.
- Boles BR, Horswill AR: **Agr-mediated dispersal of *Staphylococcus aureus* biofilms.** *PLoS Pathog* 2008, **4**:e1000052.
- Moscoso M, Garcia E, Lopez R: **Biofilm formation by *Streptococcus pneumoniae*: role of choline, extracellular DNA, and capsular polysaccharide in microbial accretion.** *J Bacteriol* 2006, **188**:7785-7795.
- Potempa J, Mikolajczyk-Pawlinska J, Brassell D, Nelson D, Thogersen IB, Englund JJ, Travis J: **Comparative properties of two cysteine proteinases (gingipains R), the products of two related but individual genes of *Porphyromonas gingivalis*.** *J Biol Chem* 1998, **273**:21648-21657.
- Mohle RB, Langemann T, Haesner M, Augustin W, Scholl S, Neu TR, Hempel DC, Horn H: **Structure and shear strength of micro-**

- bial biofilms as determined with confocal laser scanning microscopy and fluid dynamic gauging using a novel rotating disc biofilm reactor. *Biotechnol Bioeng* 2007, **98**:747-755.
38. Kato T, Kawai S, Nakano K, Inaba H, Kuboniwa M, Nakagawa I, Tsuda K, Omori H, Ooshima T, Yoshimori T, Amano A: **Virulence of *Porphyromonas gingivalis* is altered by substitution of fimbria gene with different genotype.** *Cell Microbiol* 2007, **9**:753-765.
 39. Hamada N, Watanabe K, Sasakawa C, Yoshikawa M, Yoshimura F, Umemoto T: **Construction and characterization of a fimA mutant of *Porphyromonas gingivalis*.** *Infect Immun* 1994, **62**:1696-1704.
 40. Davey ME, Duncan MJ: **Enhanced biofilm formation and loss of capsule synthesis: deletion of a putative glycosyltransferase in *Porphyromonas gingivalis*.** *J Bacteriol* 2006, **188**:5510-5523.
 41. Nakao R, Senpuku H, Watanabe H: ***Porphyromonas gingivalis* galE is involved in lipopolysaccharide O-antigen synthesis and biofilm formation.** *Infect Immun* 2006, **74**:6145-6153.
 42. Chen W, Honma K, Sharma A, Kuramitsu HK: **A universal stress protein of *Porphyromonas gingivalis* is involved in stress responses and biofilm formation.** *FEMS Microbiol Lett* 2006, **264**:15-21.
 43. Burgess NA, Kirke DF, Williams P, Winzer K, Hardie KR, Meyers NL, Aduse-Opoku J, Curtis MA, Camara M: **LuxS-dependent quorum sensing in *Porphyromonas gingivalis* modulates protease and haemagglutinin activities but is not essential for virulence.** *Microbiology* 2002, **148**:763-772.
 44. Chung WO, Park Y, Lamont RJ, McNab R, Barbieri B, Demuth DR: **Signaling system in *Porphyromonas gingivalis* based on a LuxS protein.** *J Bacteriol* 2001, **183**:3903-3909.
 45. James CE, Hasegawa Y, Park Y, Yeung V, Tribble GD, Kuboniwa M, Demuth DR, Lamont RJ: **LuxS involvement in the regulation of genes coding for hemin and iron acquisition systems in *Porphyromonas gingivalis*.** *Infect Immun* 2006, **74**:3834-3844.
 46. Yuan L, Hillman JD, Progulsk-Fox A: **Microarray analysis of quorum-sensing-regulated genes in *Porphyromonas gingivalis*.** *Infect Immun* 2005, **73**:4146-4154.
 47. Chen W, Palmer RJ, Kuramitsu HK: **Role of polyphosphate kinase in biofilm formation by *Porphyromonas gingivalis*.** *Infect Immun* 2002, **70**:4708-4715.
 48. Nagata H, Murakami Y, Inoshita E, Shizukuishi S, Tsunemitsu A: **Inhibitory effect of human plasma and saliva on co-aggregation between *Bacteroides gingivalis* and *Streptococcus mitis*.** *J Dent Res* 1990, **69**:1476-1479.
 49. Palmer RJ Jr, Kazmerzak K, Hansen MC, Kolenbrander PE: **Mutualism versus independence: strategies of mixed-species oral biofilms in vitro using saliva as the sole nutrient source.** *Infect Immun* 2001, **69**:5794-5804.
 50. Kuboniwa M, Tribble GD, James CE, Kilic AO, Tao L, Herzberg MC, Shizukuishi S, Lamont RJ: ***Streptococcus gordonii* utilizes several distinct gene functions to recruit *Porphyromonas gingivalis* into a mixed community.** *Mol Microbiol* 2006, **60**:121-139.
 51. Kuboniwa M, Amano A, Kimura KR, Sekine S, Kato S, Yamamoto Y, Okahashi N, Iida T, Shizukuishi S: **Quantitative detection of periodontal pathogens using real-time polymerase chain reaction with TaqMan probes.** *Oral Microbiol Immunol* 2004, **19**:168-176.

Publish with **BioMed Central** and every scientist can read your work free of charge

"BioMed Central will be the most significant development for disseminating the results of biomedical research in our lifetime."

Sir Paul Nurse, Cancer Research UK

Your research papers will be:

- available free of charge to the entire biomedical community
- peer reviewed and published immediately upon acceptance
- cited in PubMed and archived on PubMed Central
- yours — you keep the copyright

Submit your manuscript here:
http://www.biomedcentral.com/info/publishing_adv.asp

